High Frequency Crosstalk Between Two Microstrip Lines

Joaquín Bernal, Francisco Mesa, and Raúl Rodríguez-Berral

Department of Applied Physics 1,
University of Seville, Seville, 41012, Spain

David R. Jackson

Department of Electrical and Computer Engineering,
University of Houston, Houston, Texas, 77204-4005, USA

Abstract — **The high-frequency crosstalk current induced on a microstrip line due to coupling from an adjacent line with a source is examined. The full-wave analysis includes the effects of leaky-mode excitation and discontinuity radiation from the source.**

I. Introduction

The full-wave calculation of the high-frequency current excited by a source on a microstrip line has recently been studied [1]. It was concluded that at high frequency, leaky-mode excitation may become significant, with the total strip current being significantly influenced by the leaky-mode current. Another type of current called the "residual-wave" current also becomes significant at high frequency [1]. Both of these currents comprise the "continuous spectrum" part of the current, which is that part of the total current that is associated with radiation, and is not predicted by a simple transmission line analysis. It was shown in [1] that significant spurious effects in the total current excited by the source may be observed, due to interference between the desired bound mode and the continuous spectrum (leaky-mode and residual-wave) current.

In this present paper, the full-wall analysis for the current excited by a source is extended to investigate the *crosstalk coupling* between a pair of microstrip lines. Crosstalk is an issue that is important in high-speed digital and analog circuits [2], particularly at high frequency where radiation effects become important. In the canonical structure that is chosen, a 1 Volt gap source is placed on one microstrip line (line 1), which is adjacent to a passive line (line 2), as shown in Fig. 1. Both lines are assumed to be of infinite extent in the z direction, of infinitesimal thickness, and perfectly conducting.

Results are presented to show how the current induced on line 2 depends on the frequency, permittivity, and line spacing. For comparison purposes, the current that is predicted by simple transmission line theory is also shown.

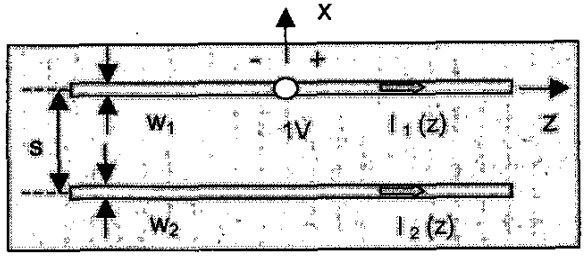

Fig. 1. Top view of coupled microstrip lines. Line 1 is excited with a 1 Volt gap source at z = 0. Line 2 is electromagnetically coupled to line 1. The substrate has a relative permittivity ε_r and a thickness h.

II. Summary of Analysis

The current is calculated on both lines using an accurate semi-analytical spectral-domain solution, in which discrete complex image theory (DCIT) is used to improve the computational efficiency [3]. The analysis accounts for all full-wave effects such as physical and nonphysical leaky-mode excitation [4] and residual-wave currents.

The current on each line is first formulated in the spectral domain, using an extension of the method presented in [1] for a source on a single line. The currents on line 1 and 2 are expressed in terms of their Fourier transforms. That is,

$$I_1(z) = \frac{1}{2\pi} \int_{C_z} \tilde{I}_1(k_z) e^{-jk_z z}\, dk_z , \qquad (1)$$

0-7803-7695-1/03/$17.00 © 2003 IEEE

$$I_2(z)=\frac{1}{2\pi}\int_{C_z}\tilde{I}_2(k_z)e^{-jk_z z}\,dk_z. \quad (2)$$

By applying Galerkin's method in the spectral domain, the Fourier transform of the strip currents on lines 1 and line 2 can be obtained as

$$\tilde{I}_1(k_z)=\frac{2\pi\,\tilde{E}_z^{gap}(k_z)}{A_{11}(k_z)-A_{12}^2(k_z)/A_{22}(k_z)} \quad (3)$$

$$\tilde{I}_2(k_z)=\frac{2\pi\,\tilde{E}_z^{gap}(k_z)}{A_{12}(k_z)-A_{22}(k_z)A_{11}(k_z)/A_{12}(k_z)} \quad (4)$$

where

$$A_{11}(k_z)=\int_{C_x}\tilde{\eta}_1^2(k_x)\tilde{G}_{zz}(k_x,k_z)\,dk_x \quad (5)$$

$$A_{22}(k_z)=\int_{C_x}\tilde{\eta}_2^2(k_x)\tilde{G}_{zz}(k_x,k_z)\,dk_x \quad (6)$$

$$A_{12}(k_z)=\int_{C_x}\tilde{\eta}_1(k_x)\tilde{\eta}_2(k_x)\tilde{G}_{zz}(k_x,k_z)\,e^{-jk_x s}dk_x. \quad (7)$$

In these equations, $\tilde{E}_z^{gap}(k_z)$ is the 1D Fourier transform of the impressed field within the gap source, $E_z^{gap}(z)$, and $\tilde{G}_{zz}(k_x,k_z)$ is the spectral-domain Green's function evaluated at $y = h$ (location of strips). The terms $\tilde{\eta}_1(k_x)$ and $\tilde{\eta}_2(k_x)$ are the 1D Fourier transforms (in x) of the functions $\eta_1(x)$ and $\eta_2(x)$, which are the normalized transverse shape functions for the currents on line 1 and line 2 (normalized so that a one Amp current exists on the strips).

The spectral-domain functions $A_{ij}(k_z)$ in the formulation can be evaluated accurately in closed form by using a 2D form of DCIT, as discussed in [3]. This allows the Fourier transform of the strip currents to be obtained in closed form from Eqs. (3) and (4).

At low frequency, transmission-line theory can be used to obtain the currents on the lines. By using an even/odd mode source decomposition, the currents are found to be

$$I_1(z)=\frac{1}{4}\left(\frac{1}{Z_0^e}e^{-jk_z^e z}+\frac{1}{Z_0^o}e^{-jk_z^o z}\right) \quad (8)$$

$$I_2(z)=\frac{1}{4}\left(\frac{1}{Z_0^e}e^{-jk_z^e z}-\frac{1}{Z_0^o}e^{-jk_z^o z}\right), \quad (9)$$

where Z_0^e and Z_0^o are the even-mode and odd-mode characteristic impedances, respectively.

III. Results

Results are shown for the case where the substrate thickness is h = 1.0 mm, and the strip widths are $w_1 = w_2 = w = h$. The substrate permittivity is ε_r = 2.2 unless otherwise noted. Results for the currents are plotted versus normalized horizontal distance z / λ_0 from the source.

Figure 2 shows a result that validates the full-wave analysis method. At the low frequency of 0.1 GHz, the currents predicted by transmission-line thoery (Eqs. (8) and (9)) agree quite well with the full-wave currents calculated from Eqs. (1) and (2).

Figures 3-5 show the current on line 2 for line separations s/h = 1, 5, and 10, at three frequencies: 1 GHz, 20 GHz, and 40 GHz. At the low frequency of 1 GHz (Fig. 3), the currents are almost identical to those predicted by transmission line theory (not shown). The current exhibits an oscillatory behavior for small s/h, due to the interference between the even-mode and odd-mode currents in Eq. (9). It is interesting to note that for large separations, the crosstalk current $I_2(z)$ approaches a linear function that increases with distance z. This can be easily explained by examining Eq. (9), which can be re-written as

$$I_2(z)=\frac{1}{4}\left(\frac{1}{Z_0^e}-\frac{1}{Z_0^o}\right)e^{-jk_z^e z}+\frac{j}{2Z_0^o}e^{-jk_z^a z}\sin\left(\Delta k_z z/2\right) \quad (10)$$

where $k_z^a=\left(k_z^e+k_z^o\right)/2$ and $\Delta k_z=k_z^e-k_z^o$.

As the separation increases, the two characteristic impedances and wavenumbers become nearly equal, so that the second term in Eq. (10) dominates and gives a nearly linear behavior.

It is noted from Figs. 4 and 5 that as the frequency increases, the crosstalk current on line 2 deviates significantly from the low-frequency behavior. Rapid oscillations are observed in the curves at high frequency, due to radiation effects. Also, it is interesting to note that the crosstalk current on line 2 actually *decreases* as the frequency increases, contrary to what might be expected (since radiation effects generally increase with frequency). This is largely due to the fact that Δk_z in Eq. (10) decreases with frequency.

Figures 6 and 7 show the current on line 2 for s/h = 10, at 20 and 40 GHz, respectively, where the total current (TC) is decomposed into its constituent parts, the bound-mode (BM) current and the continuous-spectrum (CS) current. At 20 GHz the crosstalk current is mainly a BM current (as it would be at even lower frequencies), although the CS current is beginning to become appreciable. At 40 GHz the majority of the total crosstalk current is the CS current, which is neglected in all transmission line calculations. Hence, a full-wave calculation is necessary to predict high-frequency crosstalk effects accurately.

Figure 8 shows the current on line 1 at various frequencies. The CS current interferes with the BM current, resulting in oscillations in the total current that increase with frequency.

Figure 9 summarizes how the crosstalk current on line 2 changes with frequency for the case s/h =10. Up to a maximum of 40 GHz, the crosstalk current on line 2 is steadily decreasing with frequency.

Figure 10 shows the same type of result as Fig. 9 for a higher substrate permittivity of ε_r = 10.8. Up to a frequency of 20 GHz, the trend is similar to that seen in Fig. 9. However, above 20 GHz the crosstalk current on line 2 increases with frequency, due to the strong CS current that is induced on the line. Hence, the high-frequency crosstalk current that is induced by radiation effects becomes more significant for higher permittivity substrates.

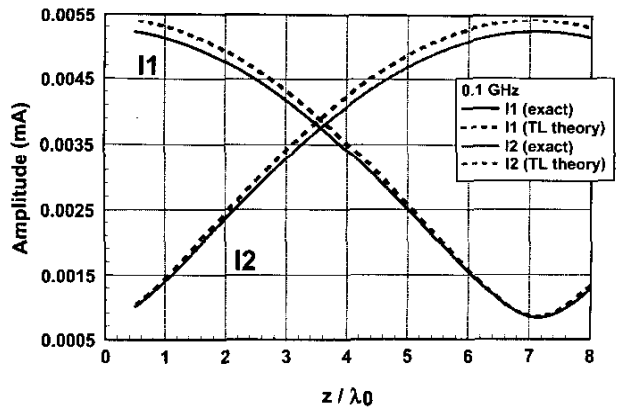

Fig. 2. Comparison of exact currents and those predicted by transmission-line theory at a low frequency of 0.1 GHz.

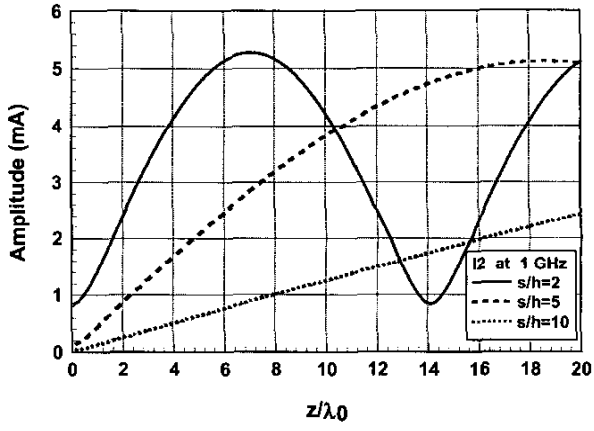

Fig. 3. Current on line 2 for various separations, at 1 GHz.

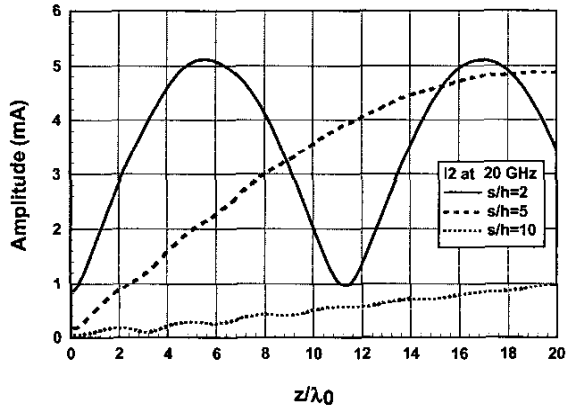

Fig. 4. Current on line 2 for various separations, at 20 GHz.

REFERENCES

[1] F. Mesa, D. R. Jackson, and M. Freire, "High Frequency Leaky-Mode Excitation on a Microstrip Line," IEEE Trans. Microwave Theory and Techniques, Vol. 49, pp. 2206-2215, Dec. 2001.

[2] B.K. Gilbert and G-W Pan, "MCM Packaging for Present- and Next-Generation High-Clock-Rate Digital- and Mixed-Signal Electronic Systems: Areas for Development," IEEE Trans. Microwave Theory and Techniques, Vol. 45, pp. 1819-1835, Oct. 1997.

[3] J. Bernal, F. Mesa, and F. Medina, "2-D Analysis of Leakage in Printed-Circuit Lines Using Discrete Complex-Images Technique," IEEE Trans. Microwave Theory and Techniques, Vol. 50, pp. 1895-1900, Aug. 2002.

[4] M. Tsuji, S. Ueki, and H. Shigesawa, "Significant Contribution of Nonphysical Leaky Mode to the Fields Excited by a Practical Source in Printed-Circuit Transmission Lines," *2002 IEEE MTT Intl. Microwave Symp. Digest*, pp. 957-960, June 2002, Seattle, WA.

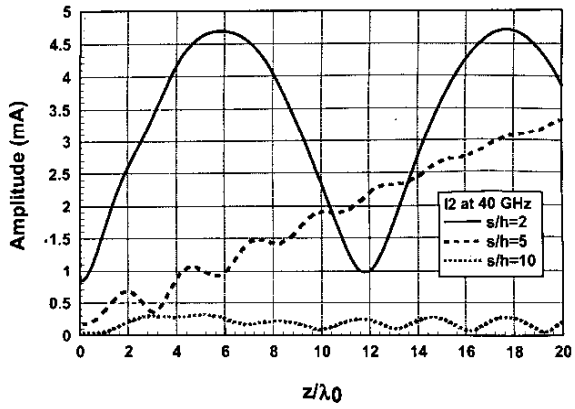

Fig. 5. Current on line 2 for various separations, at 40 GHz

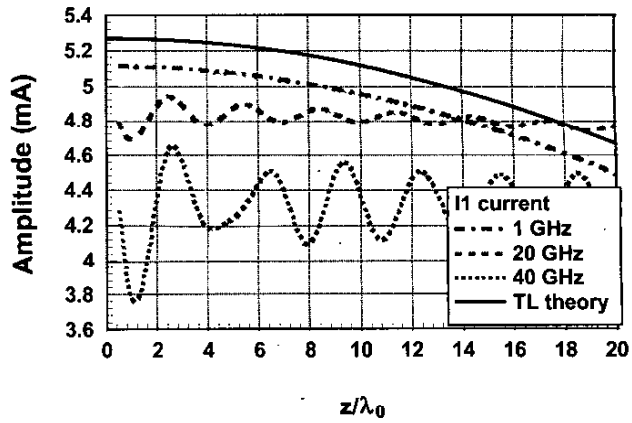

Fig. 8. Current on line 1 at various frequencies, for $s/h = 10$.

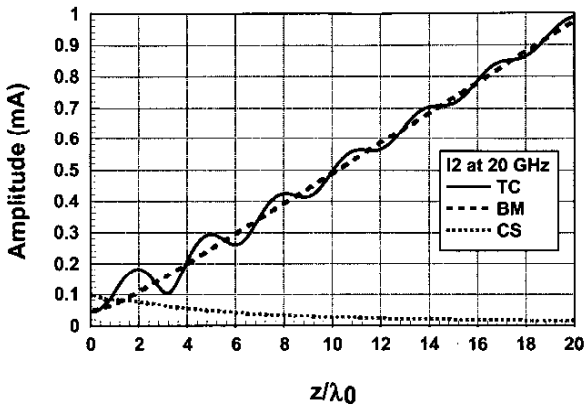

Fig. 6. Current on line 2 for $s/h = 10$, at 20 GHz

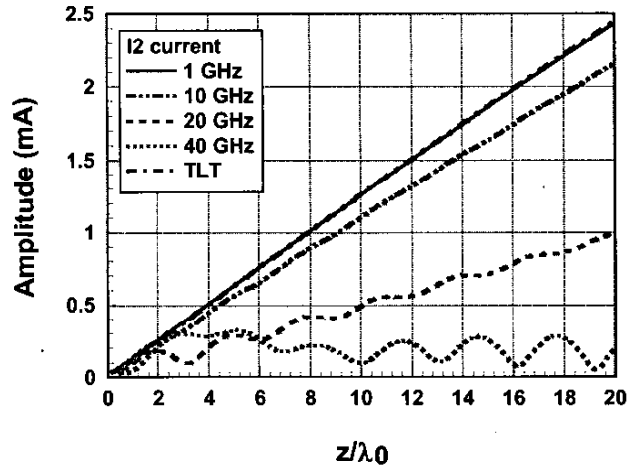

Fig. 9. Current on line 2 at various frequencies, for $s/h = 10$.

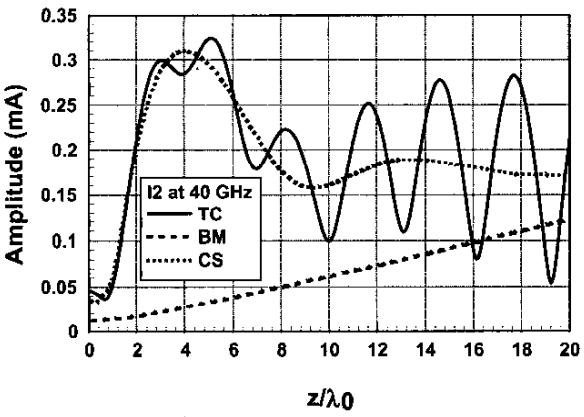

Fig. 7. Current on line 2 for $s/h = 10$, at 40 GHz

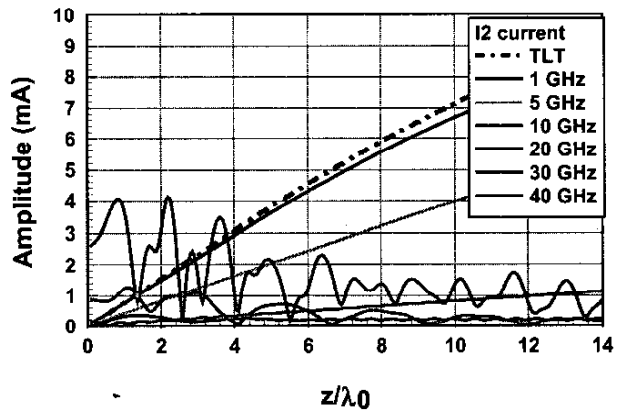

Fig. 10. Current on line 2 at various frequencies, for $s/h = 10$. A high substrate permittivity of $\varepsilon_r = 10.8$ is used.